

# Atmospheric neutrinos, long-baseline neutrino beams and the precise measurement of the neutrino oscillation parameters

Giuseppe Battistoni<sup>1</sup> and Paolo Lipari<sup>2</sup>

1. *I.N.F.N., Sezione di Milano, via Celoria 16, I-20133 Milano, Italy*

2. *Dipartimento di Fisica, Università di Roma "la Sapienza", and  
I.N.F.N., Sezione di Roma, Piazzale A. Moro 2, I-00185 Roma, Italy*

## Abstract

Measurements of atmospheric neutrinos by Super-Kamiokande and other detectors have given evidence for the existence of neutrino oscillations with large mixing and  $\Delta m^2$  in the range  $10^{-3}$ – $10^{-2}$  eV<sup>2</sup>. In this work we discuss critically some of the possible experimental strategies to confirm this result and determine more accurately the neutrino oscillation parameters. A possible method is the development of long-baseline accelerator neutrino beams. The accelerator beams can have higher intensity and higher average energy than the atmospheric flux, and if  $\nu_\mu \leftrightarrow \nu_\tau$  oscillations are indeed the cause of the atmospheric neutrino anomaly, they can produce a measurable rate of  $\tau$  leptons for most (but not all) of the values of the oscillation parameters that are a solution to the atmospheric data. On the other hand measurements of atmospheric neutrinos with large statistics and/or better experimental resolutions, can also provide convincing evidence for oscillations, thanks to unambiguous detectable effects on the energy, zenith angle and  $L/E_\nu$  distributions of the events. The study of these effects can provide a precise determination of the oscillations parameters. The range of  $L/E_\nu$  available for atmospheric neutrinos is much larger than in long-baseline accelerator experiments, and the sensitivity extends to lower values of  $\Delta m^2$ .

*To appear in the proceedings of the 1998 "Vulcano Workshop on Frontier objects in Astrophysics and Particle Physics".*

# 1 Introduction

The data of Super-Kamiokande [1] has strengthened the evidence for the existence of an anomaly in the flavor ratio of atmospheric neutrinos. The indication for the existence of neutrino oscillation has originally appeared [2] as the measurement of a ratio  $R_{\mu/e}$  of  $\mu$ -like and  $e$ -like events lower than the MC expectation. The high statistics data of Super-Kamiokande show distortions of the angular distributions of sub-GeV and multi-GeV  $\mu$ -like that strongly support the neutrino oscillation hypothesis. The angular distribution of the  $e$ -like events is consistent with the no-oscillation hypothesis, in agreement with the results with the reactor experiment Chooz [3] that essentially rules out the  $\nu_e \leftrightarrow \nu_x$  oscillations in the interesting region of parameter space. It is clear that it is necessary to confirm in an unambiguous way if neutrino oscillations are indeed the cause of the effects seen in the atmospheric neutrino experiments. If this will turn out to be the case, the next task is to measure with great accuracy the oscillation parameters.

At present, the scientific community is discussing about the best experimental strategy to accomplish this task. Long-baseline (LBL) neutrino experiments are being designed for this purpose, but there is also a strong debate on the role of possible new atmospheric neutrino detectors different from Super-Kamiokande. The main problem is the fact that the region of oscillation parameters suggested by the Super-Kamiokande data ( $0.5 \leq |\Delta m^2|/10^{-3} \text{ eV}^2 \leq 6$  at 90% confidence level) is lower than previous estimates, and the planned LBL experiments could fail in achieving their goal of the unambiguous detection or the ruling out of flavor oscillations as explanation of the atmospheric neutrino problem.

The purpose of this work is to discuss and compare the potential in proving unambiguously the existence of oscillations and in the determination of the oscillation parameters, of both long-baseline (LBL) neutrino beams and of higher statistics and/or higher quality measurements of atmospheric neutrinos. For the sake of clarity and simplicity we will limit our discussion to the simplest solution for the problem, namely the existence of  $\nu_\mu \leftrightarrow \nu_\tau$  oscillations. A general analysis in terms of a 3-neutrino scheme, or considering also the possibility of mixing with light sterile states is of course desirable, and should be considered in a more complete discussion.

The  $\nu_\mu \leftrightarrow \nu_\tau$  oscillation probability for neutrinos propagating in ordinary matter is given by the well known formula:

$$P_{\nu_\mu \rightarrow \nu_\tau} = \sin^2 2\theta \sin^2 \left( \frac{\Delta m^2}{4} \frac{L}{E_\nu} \right) \quad (1)$$

For small values of  $L/E_\nu$ , ( $L/E_\nu \ll |\Delta m^2|^{-1}$ ) expanding the second sine in eq.(1) the oscillation probability can be approximated as:

$$P_{\nu_\mu \rightarrow \nu_\tau} \simeq \sin^2 2\theta (\Delta m^2)^2 \frac{L^2}{16} \frac{1}{E_\nu^2} \quad (2)$$

note that the two parameters  $\sin^2 2\theta$  and  $\Delta m^2$  appear as a single multiplicative factor in the combination  $\sin^2 2\theta (\Delta m^2)^2$  and cannot be measured separately.

This work is organized as follows: in the next section we discuss the properties of the atmospheric neutrino flux and of the proposed LBL beams, including a short analysis of systematic uncertainties in the calculation of no-oscillation predictions. Then we discuss the signatures of neutrino oscillations on observable quantities, considering separately “appearance” and “disappearance” for LBL neutrinos. We then discuss the potential of atmospheric neutrino measurements. A summary and discussion follow.

## 2 Atmospheric and Accelerator Neutrino Beams

In fig. 1 we compare the energy spectrum of atmospheric neutrinos with the predicted spectra for three long-baseline beams: (i) KEK to SuperKamiokande (K2K) [4] (proton energy  $E_0 = 12$  GeV, neutrino path-length  $L \simeq 250$  km, intensity  $N_p = 3.3 \times 10^{19}$  yr $^{-1}$ ), (ii) Fermilab to MINOS [5] ( $E_0 = 120$  GeV,  $L \simeq 730$  km,  $N_p = 2.0 \times 10^{20}$  yr $^{-1}$ ) and (iii) CERN to Gran Sasso laboratory [6] ( $E_0 = 400$  GeV,  $L \simeq 730$  km,  $N_p = 3.0 \times 10^{19}$  yr $^{-1}$ ). To estimate the proton intensities of the Fermilab and CERN beams we have used for both cases the predicted repetition rate of the accelerator and considered a year of 220 days of running with an efficiency of 50%. The event rates plotted in fig. 1 are calculated in the absence of neutrino oscillations, and refer to charged current (CC) interactions of  $\nu_\mu$ ’s in the case of the accelerator beams, and  $(\nu_\mu + \bar{\nu}_\mu)$ ’s or  $(\nu_e + \bar{\nu}_e)$ ’s for atmospheric neutrinos. In all cases we have used the same description of the neutrino cross section from [7]. The atmospheric neutrino event rate was calculated using the Bartol [8] or Honda et al. [9] neutrino flux for the geomagnetic location of Kamiokande. The event rates are plotted on an absolute scale (in (kton yr) $^{-1}$ ), but to make the plot more readable we have rescaled the KEK, Fermilab and CERN beams with factors of 5, 0.1 and 0.1. Note that fig. 1 we plot as a function of the logarithms of the energy the distribution  $dN_\nu^{cc}/d\log E_\nu$ , therefore the total rate is proportional to the area under the curves or histograms<sup>1</sup>.

Neutrino oscillations (in the absence of matter effects) are a function of the parameter  $L/E_\nu$  and it is therefore interesting to show the event rate as a function of this quantity. This is done in fig. 2 where we plot the event rates for atmospheric neutrinos and for the 3 LBL experiments plotted as a function of the parameter  $L/E_\nu$ . The event rates are calculated as in fig. 1 and are for CC interactions. In the case of atmospheric neutrinos the rate is for muon (anti)-neutrinos and we have also included the requirement that the final state  $\mu^\pm$  has a momentum  $p_\mu > 200$  MeV.

In the upper panel of fig. 2 we show an example of the oscillation probability (eq.1) with values of the parameters  $\sin^2 2\theta = 1$  and  $\Delta m^2 = 3 \times 10^{-3}$  eV $^2$ . The oscillation parameters of this example are chosen as ‘typical’ values obtained as solution of the neutrino atmospheric anomaly, close to the point of minimum  $\chi^2$  for the combined sub-GeV and multi-GeV data of the SuperKamiokande detector [1] ( $\Delta m^2 = 2.2 \times 10^{-3}$  eV $^2$ ,  $\sin^2 2\theta = 1$ ). Previous data of the Kamiokande experiment [10] suggested a higher best

---

<sup>1</sup>We find that this representation of the spectrum is in most cases more useful than the commonly used plot of  $dN_\nu/dE_\nu$  with a linear energy scale. For example looking at fig. 1 one can easily read the fraction of the event rate with  $E_\nu \leq 10$  GeV (or  $E_\nu \geq 100$  GeV).

fit value  $\Delta m^2 \simeq 1.5 \times 10^{-2} \text{eV}^2$ .

Integrating over all values of  $L/E_\nu$  the event rates for atmospheric neutrinos, and for the K2K, Fermilab and CERN experiments are  $N_\mu = 140, 21, 2100$  and  $1530 \text{ (kton yr)}^{-1}$ . The two proposed high energy experiment obviously benefit from having a large event rate, 10 to 15 times higher than atmospheric neutrinos.

Atmospheric neutrinos arrive from all directions including up-going trajectories that have crossed the earth have a very broad range of path-lengths  $L \simeq 10\text{--}10^4 \text{ km}$  that is reflected in a broad range of  $L/E \simeq 1\text{--}10^5 \text{ km/GeV}$ . The plot of the event rate as a function of  $L/E_\nu$  has a characteristic two-bumps form, that correspond to down-going and up-going particles. The ‘valley’ in between is populated mostly by particles with directions close to the horizontal, the event rate per unit  $L/E_\nu$  is lower in this region because the path-length  $L$  changes rapidly with the variation of the neutrino zenith angle  $\theta_z$ . For accelerator neutrinos the path-length  $L$  is fixed (the width of the region where neutrinos are produced  $\Delta L \lesssim 1 \text{ km}$  being much smaller than  $L$ ) and the distribution in  $L/E_\nu$  reflects the energy spectrum of the neutrinos (using a logarithmic scale the  $L/E_\nu$  distribution is simply the energy distribution translated and reflected). The two high energy accelerator experiments have the same  $L$  and the difference between the two distributions reflects the lower energy and higher intensity of the Fermilab accelerator. The K2K experiment has a much lower intensity, was carefully designed to send a controlled flux of accelerator-made neutrinos in precisely the range of values of  $L/E_\nu$  where neutrino oscillations with parameters suggested by the Kamiokande experiment would have the greatest visible effects.

Comparing the lower and upper panel of fig. 2 it can be noticed the high energy LBL beams of Fermilab and Minos will have a limited sensitivity to oscillations with  $\Delta m^2 \lesssim 3 \times 10^{-3} \text{ eV}^2$  because of the small expected event rate  $L/E_\nu \gtrsim 100 \text{ km/GeV}$ . The probability  $P_{\nu_\mu \rightarrow \nu_\mu}$  has minima for values  $L/E_\nu = n (L/E_\nu)^*$  where  $n$  is an integer. The first minimum occurs at

$$\left(\frac{L}{E}\right)^* = \frac{2\pi}{\Delta m^2} = \frac{1236}{\Delta m_{-3}^2} \text{ km/GeV} \quad (3)$$

where  $\Delta m_{-3}^2$  is the value of the squared mass difference in units of  $10^{-3} \text{ eV}^2$ . It is clearly very desirable to measure the neutrino oscillation probability up to values of  $L/E_\nu$  that approach and exceed  $(L/E)^*$ . If this is not achieved, the value of the mixing parameter  $\sin^2 2\theta$  that gives the depth of the minimum in the survival probability cannot be measured, and in fact the phenomenon of neutrino *oscillations* cannot be experimentally proven.

In LBL experiments the path-length  $L$  is fixed and the  $P_{\nu_\mu \rightarrow \nu_\mu}$  probability has minima for  $E_\nu = E^*/n$  with  $E^* = \Delta m^2 L / (2\pi)$ . For the proposed LBL experiments the highest energy minimum is:

$$E^*(\text{K2K}) = 0.20 \Delta m_{-3}^2 \text{ GeV} \quad (4)$$

$$E^*(\text{CERN}) = 0.59 \Delta m_{-3}^2 \text{ GeV} \quad (5)$$

For the Fermilab experiment the no-oscillation CC event rates with  $E_\nu$  below 10, 5 and 2 GeV are 420, 50 and 2.5 events per year. For the present design of the CERN beam with

lower intensity and the focus optimized for higher energies, the event rates are roughly 34, 3.5 and  $0.5 \text{ yr}^{-1}$ . Given these rates the  $L/E_\nu$  region where one expects the survival (transition) probability to have a minimum (maximum) appears to be accessible only for the high values of  $\Delta m^2$  in the range suggested by the atmospheric neutrino data.

It is possible to prove the existence of flavor transitions without having neutrinos with  $L/E_\nu$  as large as  $(L/E)^*$ . In this case only the product  $\sin^2 2\theta (\Delta m^2)^2$  is experimentally measurable. For  $\Delta m^2 \lesssim 10^{-2} \text{ eV}^2$  this is what will happen with the proposed LBL neutrino beams.

## 2.1 Atmospheric neutrinos

Detailed calculations of atmospheric neutrino fluxes can be found in literature. At present, two of the most quoted results are those of Honda et al. [9] and those of the Bartol group [8]. These neutrino flux calculations are based on a unidimensional description of the c.r. showers. Recent comparisons with a 3-dimensional calculation based on the FLUKA montecarlo [11] confirm that the approximation is adequate at least for neutrinos above 200 MeV.

We refer to the quoted references for the description of the main features of atmospheric neutrinos. Here we limit ourselves to focus some important properties which are relevant in the search for oscillations and that can be predicted very reliably.

1. The neutrino fluxes are to a very good approximation up-down symmetric:

$$\phi_{\nu_\alpha}(E, \cos \theta_z) = \phi_{\nu_\alpha}(E, -\cos \theta_z) \quad (6)$$

2. The electron neutrino and muon neutrino fluxes originate from the decay of the same charged mesons, and are strictly related to each other:

$$\phi_{\nu_e + \bar{\nu}_e}(E, \cos \theta_z) = r_{e\mu} \phi_{\nu_\mu + \bar{\nu}_\mu}(E, \cos \theta_z) \quad (7)$$

where the factor  $r_{e\mu}$  is only weakly dependent on the neutrino energy and direction and close to  $\frac{1}{2}$ .

Geomagnetic effects introduce at low energy a small violation of the up-down symmetry. of order of  $\sim 10\%$  for the ‘sub-GeV’ sample of SuperKamiokande, but in the absence of oscillations the relation (6) can be reliably predicted as valid with few percent accuracy above 1 GeV [12]. The size of the geomagnetic effects on neutrinos can also be measured observing a small east-west effect [12] that is approximately independent from oscillations. No mechanism besides neutrino oscillations, has been proposed to explain the large deviation observed from the up-down symmetry observed in the multi-GeV data of SuperKamiokande.

The deviation of the measured  $e$ -like/ $\mu$ -like ratio from the expected value has been the origin of the atmospheric neutrino problem. In the presence of  $\nu_\mu \rightarrow \nu_x$  oscillations with  $x \neq e$  the electron neutrino flux can be a quite accurate monitor of the no-oscillation flux.

## 2.2 Long baseline accelerator neutrino beams

It can be useful to have a qualitative understanding of the intensity and energy distribution of a long baseline accelerator beam. To a good approximation (a more complete discussion is contained in the appendix) the energy distribution of the flux of neutrinos at the far detector is given by the following formula:

$$\frac{dN_\nu}{dE_\nu}(E_\nu) \simeq \frac{N_p}{4\pi L^2} \left\{ 2.34 \left[ \frac{dn_\pi}{dE_\pi}(E_\pi, E_0) P_{dec}^\pi(E_\pi) \right]_{E_\pi=2.34 E_\nu} \frac{E_\nu^2}{\langle p_{\perp\nu}^\pi(E_\nu) \rangle^2} + 1.05 \left[ \frac{dn_K}{dE_K}(E_K, E_0) P_{dec}^K(E_K) \right]_{E_K=1.05 E_\nu} \frac{E_\nu^2}{\langle p_{\perp\nu}^K(E_\nu) \rangle^2} \right\} \quad (8)$$

where  $E_0$  and  $N_p$  are the energy and intensity (particles per unit time) of the primary proton beam,  $L$  is the distance between accelerator and detector,  $dn_\pi/dE_\pi$  ( $dn_K/dE_K$ ) is the inclusive energy distribution of positive pions (kaons) in the final state, and  $P_{dec}^{\pi(K)}(E_\pi)$  is the decay probability in the  $\mu\nu_\mu$  final state of charged pions and kaons that depends on the dimensions of the decay volume after the interaction region (in the case of the kaons one has also to include the branching fraction  $B_{K \rightarrow \mu\nu} \simeq 0.64$ ). The numerical factors  $2.34 = m_\pi^2/(m_\pi^2 - m_\mu^2)$  and  $1.05 = m_K^2/(m_K^2 - m_\mu^2)$  are due to the fact that the neutrinos produced in the direction parallel to parent particle momentum in the  $\mu\nu$  decay of a relativistic pion (kaon) have momentum  $E_\nu = E_\pi/2.34$  ( $E_\nu = E_K/1.05$ ). Because of this kinematical reason, the neutrinos produced in pion (kaon) decay have a spectrum that extends up to different maximum energy. The factor  $E_\nu^2/\langle p_{\perp\nu} \rangle^2$  is due to the fact that the intensity of the neutrino flux is more intense when the neutrinos are emitted in a small solid angle. Note that the transverse momentum of the neutrinos has a contribution due to the  $p_\perp$  obtained in the decay of the parent particle, and a contribution due to the  $p_\perp$  of the parent particle:

$$p_{\perp\nu} = p_{\perp}^{\pi \rightarrow \nu} \oplus p_{\perp}^\pi \quad (9)$$

The second contribution can be reduced optimizing the focusing downstream of the target, while the first one is unavoidable. Since the maximum transverse momentum in a pion (kaon) decay is 29.8 (236) MeV, the contribution of the kaons is suppressed with respect to the pion one.

In the approximation of ‘perfect-focus’ it is assumed that all charged mesons of the appropriate charge and positive longitudinal momentum, after the focusing system have the 3-momentum parallel to the primary proton beam (that is  $p_{\perp}^{\pi,K} \equiv 0$ ), neglecting also secondary interactions and decays before or during the magnetic bending. In this case (see eq.32) it is possible to deduce the validity of formula (8) rigorously. More in general all details of the focusing system are absorbed in the definition of  $\langle p_{\perp}^{\pi,K}(E) \rangle$ .

The number of pions of energy  $E_\pi$  produced in an interaction by a primary proton of energy  $E_0$  is well represented by the scaling expression:

$$\frac{dn_\pi}{dE_\pi}(E_\pi, E_0) \simeq \frac{1}{E_\pi} F\left(\frac{E_\pi}{E_0}\right) \quad (10)$$

where the function  $F(x)$  is approximately independent from the primary energy  $E_0$ , and decreases monotonically from a finite value for  $x \rightarrow 0$ , to zero for  $x \rightarrow 1^2$ . Therefore the number of pions at *all* energies increases with increasing  $E_0$ . The known and observed violations of the scaling expressed by Equation (10), result in a higher rapidity plateau and in more rapidly increase of the multiplicity of low energy pions and kaons.

We can make some general considerations on the flux

1. The neutrino flux grows linearly with the intensity of the proton beam, and decreases with distance as  $L^{-2}$ .
2. In the perfect focus approximation at low energy the spectrum of the neutrinos is approximately the form  $\phi_\nu \propto E_\nu$ , and the energy distribution of the interacting neutrinos is  $dN_{int}/dE_\nu \propto E_\nu^2$ .
3. Increasing the energy  $E_0$  of the proton beam, for the same target and focusing configuration, the neutrino flux increases for all neutrino energies  $E_\nu$  (and not only for the highest energies). However one should also consider the fact that the intensity of the proton beam can increase to the shorter time needed to accelerate protons at a lower energy.

In fig. 5 we show a calculation of the rate of CC interactions  $\phi_{\nu_\mu}(E_\nu; E_0, L) \sigma_{CC}^{\nu_\mu}$  calculated under the approximation of perfect focusing (equation (32)) for  $L = 730$  km and  $E_0 = 120$  and 400 GeV and compare with the results of the complete Montecarlo simulations of the Fermilab and CERN LBL beams. For the decay probability we have considered a decay tunnel of length  $T$  and a large transverse section. Then  $P_{dec}(E_a) = 1 - \exp[-\varepsilon_a/(\beta E_a)]$ , with  $\varepsilon_a = m_a T/\tau_a$ . For  $T = 800$  m  $\varepsilon_{\pi(K)} = 14.3$  (106.5) GeV. For the lowest energy (120 GeV) we also show the contribution of  $\pi^+$  (dot-dashed) and  $K^+$  (dashed line). The kaon contribution extends to higher energy because a neutrino emitted in the forward direction in a kaon decay has energy  $E_\nu = 0.954 E_K$  while in a pion decay the neutrinos get at most a fraction 0.427 of the parent energy. The kaon contribution is suppressed with respect to the pion's one because of the larger  $p_\perp$  available in the decay, but enhanced at large energy because of the shorter lifetime.

### 2.2.1 Optimization of LBL neutrino beams

The construction of a LBL neutrino beam involves choices for  $L$ , the distance between the accelerator and the detector,  $E_0$  the energy of the primary proton beam, and the detailed design of the target and magnetic focusing system.

Of course there are technical and ‘financial’ constraints on the design, for example the choice of  $L$  is strongly limited by the location of the existing particle accelerators and the possible sites for the neutrino detector. The ‘optimum’ design of the neutrino beam depends on the channel of oscillations that is searched for (for example  $\nu_\mu \rightarrow \nu_\tau$  or  $\nu_\mu \rightarrow \nu_e$ ), the the region of parameter space that is searched for oscillations (for example

---

<sup>2</sup>Very roughly  $F(x) \sim (1 - x)^4$ .

large or small  $|\Delta m^2|$ ), and the experimental strategy used in the search (for example ‘appearance’ and ‘disappearance’ experiments).

Therefore if several detectors using different techniques or having different aims are planning to use the same neutrino beam, it will be necessary to find a compromise solution between different optimum designs. Ideally the design of the neutrino beam and of the detectors (and their search strategies) should be developed at the same time.

A quantity that is often quoted in the discussion of the design of a neutrino beam is the rate of charged current muon neutrino interactions expected in the absence of oscillations ( $N_\mu^\circ$ ):

$$N_\mu^\circ = \int dE_\nu \phi_{\nu_\mu}^\circ(E_\nu) \sigma_{\nu_\mu}(E_\nu) \quad (11)$$

It should be stressed that the optimization of the neutrino beam in general does *not* coincide with the maximization of  $N_\mu^\circ$ .

For example, in the case of experiments that are searching for the appearance of  $\tau$  leptons, a more interesting quantity is the rate  $N_\tau$  of charged current interactions of  $\nu_\tau$ <sup>3</sup>. The rate  $N_\tau$  depends of course on the oscillation parameters:

$$N_\tau(\Delta m^2, \sin^2 2\theta) = \int dE_\nu \phi_{\nu_\mu}^\circ(E_\nu) P_{\nu_\mu \rightarrow \nu_\tau}(E_\nu, \Delta m^2, \sin^2 2\theta) \sigma_{\nu_\tau}(E_\nu) \quad (12)$$

It is interesting to discuss the form that this equation takes in the limits of very large or very small  $|\Delta m^2|$ , or more precisely for  $|\Delta m^2| L/E_\nu$  much greater (smaller) than unity.

In the limit of large  $|\Delta m^2|$ , averaging over the rapid oscillations the transition probability takes an energy independent constant value  $P_{\nu_\mu \rightarrow \nu_\tau} \simeq \frac{1}{2} \sin^2 2\theta$  and we have:

$$N_\tau \simeq \frac{\sin^2 2\theta}{2} n_\tau^\infty \quad (13)$$

where

$$n_\tau^\infty = \int dE_\nu \phi_{\nu_\mu}^\circ(E_\nu) \sigma_{\nu_\tau}(E_\nu) = \frac{\langle \sigma_{\nu_\tau} \rangle}{\langle \sigma_{\nu_\mu} \rangle} N_\mu^\circ \quad (14)$$

$\langle \sigma_{\nu_{\tau(\mu)}} \rangle$  is the charged current  $\nu_\tau$  ( $\nu_\mu$ ) cross section averaged over the neutrino flux spectrum.

In the limit of small  $|\Delta m^2|$  the oscillation probability can be approximated with the form of eq.(2) and the rate of  $\tau$  production becomes:

$$N_\tau \simeq \sin^2 2\theta (\Delta m^2)^2 n_\tau^0 \quad (15)$$

with

$$n_\tau^0 = \frac{L^2}{16} \int dE_\nu \frac{\phi_{\nu_\mu}^\circ(E_\nu)}{E_\nu^2} \sigma_{\nu_\tau}(E_\nu) \quad (16)$$

There are several points that are worth discussing about equations (15,16) and the limit of small  $|\Delta m^2|$ :

---

<sup>3</sup>For a realistic discussion one should also include a discussion of an energy dependent detection efficiency, and also the possible sources of background.



1. The limit of small  $|\Delta m^2|$  is to a good approximation valid for the planned LBL neutrino beams and the range of  $|\Delta m^2|$  indicated by Super-Kamiokande.
2. In this limit the rate of  $\tau$  production grows linearly with  $\sin^2 2\theta$  and *quadratically* with  $|\Delta m^2|$ .
3. The oscillation parameters enter in the rate as a single energy dependent multiplicative factor:  $R_\tau \propto \sin^2 2\theta (\Delta m^2)^2$ . Therefore the two parameters cannot be disentangled from each other.
4. In the evaluation of the quantity  $n_\tau^0$  (equation (16)) each neutrino energy is weighted by the intensity of the flux, the cross section for  $\tau$  production and an additional factor  $E_\nu^{-2}$  that takes into account the oscillation probability that decreases with increasing energy. The most ‘useful’ neutrino energies are those not much higher than the  $\tau$ -lepton threshold. The optimum spectrum is significantly softer than one optimized spectrum for a search for  $\tau$  appearance at large  $|\Delta m^2|$ .
5. The measurement of the combination  $\sin^2 2\theta (\Delta m^2)^2$  depends on the measurement of the *absolute* rate of  $\tau$ -production. Therefore uncertainties on the absolute value of the  $\nu_\tau$  cross section, the detection efficiency and the neutrino flux intensity are important sources of systematic uncertainty.
6. The rate  $N_\tau$  is *independent* on  $L$ . The neutrino flux at the far detector decreases as  $L^{-2}$  because of the divergence of the beam, but the oscillation probability grows proportionally to  $L^2$ . The resulting rate is independent from  $L$ .

For disappearance experiments one has to maximize the rate difference  $\Delta N_\mu = N_\mu^\circ - N_\mu$  between the observed rate and the no-oscillation rate, or the ratio  $\Delta R_\mu / R_\mu^\circ$ . The crucial region is the one to the energy

$$E^* = \frac{\Delta m^2 L}{2\pi} = 0.59 \left( \frac{L}{730 \text{ km}} \right) \left( \frac{|\Delta m^2|}{10^{-3} \text{ eV}^2} \right) \text{ GeV} \quad (17)$$

Neutrinos with energy  $E_\nu \gg E^*$  do not oscillate and therefore are useless in the search for oscillations and a potential source of background.

Summarizing, the optimization of a neutrino beam depends on the experiment one wants to perform. This poses some difficult problems if experiments with different goals or using different strategies want to use the same beam. A neutrino beam optimized for a short-baseline  $\nu_\tau$  appearance experiment such as COSMOS or TOSCA will have higher energy than a beam optimized for the ICARUS or OPERA experiments searching for oscillations at low  $|\Delta m^2|$ . The sensitivity of a disappearance experiment is optimized constructing a neutrino beam of still lower energy.

### 2.3 Uncertainties in the calculation of the $\nu$ beams

Comparing the LBL accelerator beams with the atmospheric flux we can note that conceptually the process of neutrino production is the same for both processes. A primary high energy hadron beam interacts with a target, and neutrinos are produced in the weak decay of final state mesons.

The primary flux is for all practical purposes exactly known in an accelerator experiment, while there are significant uncertainties in the normalization ( $\sim 15\%$ ) and energy dependence of the primary cosmic ray (c.r.) flux (see [13] for a detailed discussion). At low energy it is also necessary to include a treatment of the solar modulation and of the geomagnetic effects. Time-varying magnetic fields in interplanetary space cause a time dependence of the c.r. primary flux at low energies. The geomagnetic field prevents the low rigidity particles from arriving at the surface of the earth, resulting in a primary flux that is not isotropic and is different for different locations. Both effects however vanish at sufficiently high energy.

Uncertainties in the modeling of particle production in hadronic showers affects the calculation of the flux for both accelerator and atmospheric neutrinos. For atmospheric neutrinos one has also to consider the interaction of nuclear projectiles (that account for a fraction of few percent of the neutrinos) and of weakly decaying mesons (a small contribution to the flux), and describe the interactions of primary particle with energy in a broad interval  $E_0 \sim 5\text{--}50$  GeV (for neutrinos with energy from 300 MeV to 2 GeV [8]. However since both the primary flux and the resulting neutrino flux are approximately isotropic only the energy distribution of the final particles is important. In the case of LBL accelerator beams also the transverse momentum distribution and the correlation between transverse and longitudinal momentum of the secondary particles is critically important. Detailed experimental studies of particle production in hadronic interactions of the appropriate energy (the beam energy for accelerator experiments and  $E_0 \sim 10\text{--}30$  GeV for atmospheric neutrinos) could reduce the uncertainties in the calculation of the neutrino spectrum and normalization.

The description of particle transport in the target and decay volume is another source of uncertainty that is important especially for accelerator neutrinos. In the case of a LBL accelerator beam the structure of the target and of the magnetic focusing system must be known and described in great detail. The detector subtends a very small solid angle and a very accurate and detailed calculation of the angular divergence of the neutrino beam as a function of energy is essential. The c.r. showers develop in a medium with small and slowly varying density. There are small uncertainties related to the time variations and geographical position dependence of the atmospheric density that in the current simulations is simply described as the average  $\rho(h)$ . The polarization of muons produced in two body decay and its effect on the spectra of neutrinos coming from chain decay as  $\pi \rightarrow \mu \rightarrow \nu$  is taken into account in the atmospheric neutrino calculations but the possible effect of muon depolarization before decay is usually neglected. This is believed to be a good approximation; in any case the main effect of the polarization is a suppression (enhancement) of the muon (electron) neutrino flux of  $\sim 10\%$ , and the uncertainty related

to this effect cannot be large.

Both for accelerator and atmospheric neutrinos there are methods to control the calculation of the no-oscillation neutrino fluxes. In an accelerator it is of course possible to construct a near detector. This is indeed an very important possibilities that is essential for any disappearance experiment. The main difficulty of this approach is that the solid angle subtended by the far detector corresponds to a region with transverse size  $\sim 1$  cm for a near detector at the distance of one kilometer, and the event rate in this region is small (by definition equal to the far detector rate). Therefore in practice the monitoring of the beam will require some assumptions about the angular distribution of the neutrinos. It is expected that beam intensity at the far detector will be approximately constant in a region of radius 100–200 meters, much larger than the detector, with a correspondingly higher tolerance in the pointing accuracy. Therefore it should be possible to use an angular region much broader than the far detector solid angle to monitor the beam in a near detector. This assumption can be, at least in part, tested experimentally. In studies of detector performance, the fact that the relevant events in the near detector are all close to the detector axis, while in the far detector are uniformly spread in the plane transverse to the beam is a potential bias that requires a correction.

In summary we would like to note that according to a rather widespread ‘common wisdom’ the systematic uncertainties on the flux of accelerator neutrinos are much smaller than for atmospheric neutrinos. This statement should be qualified because is not in general correct. In an accelerator there is the possibility of a close detector, and of sophisticated monitoring systems. In atmospheric neutrinos one can use the up-down symmetry and the relation between the  $\nu_\mu$  and  $\nu_e$  fluxes as essentially model independent tools to estimate the no-oscillation rates.

### 3 Appearance Experiments

In some sense the most convincing evidence for the existence of neutrino flavor oscillations is the positive identification of the charged current interactions of  $\tau$  neutrinos in the detector. The unambiguous detection of such events would be unquestionable proof of oscillations, since direct production of  $\nu_\tau$ ’s is predicted (and indeed measured by CHORUS and NOMAD) to be negligibly small.

In fig. 3 we show as a function of  $\Delta m^2$  the event rate of charged current  $\nu_\tau$  interactions calculated assuming the existence of  $\nu_\mu \leftrightarrow \nu_\tau$  oscillations with maximal mixing. The different curves are for atmospheric neutrinos and for the reference beams of the Fermilab and CERN long baseline projects. Essentially all neutrinos in the K2K project are below threshold for  $\tau$  production and the  $\tau$ -event rate is vanishingly small in this case..

The rate of  $\tau$  production by atmospheric neutrinos remains small, of order 1–2 events per (kiloton yr) even in the presence of large mixing between muon and tau neutrinos. This is a consequence of the fact that atmospheric neutrinos have a soft spectrum and only a small fraction is above the energy threshold for  $\tau$  production.

The high energy beams of Fermilab and CERN can provide a significant rate of  $\tau$ ’s.

Looking at fig. 3 one can distinguish three regions of  $|\Delta m^2|$  where the rate of  $\tau$  production (for a constant value of the mixing parameter) has a different behaviour:

1. for  $|\Delta m^2| \lesssim 10^{-2} \text{ eV}^2$  the rate grows as  $N_\tau \propto (\Delta m^2)^2$ ,
2. in an intermediate region it oscillates
3. for large  $|\Delta m^2|$  becomes a constant.

For the same number of protons on target the yield of  $\tau$ -events for the Fermilab and CERN reference beams in the high  $|\Delta m^2|$  region is well described by:

$$\left(\frac{N_\tau}{N_p}\right)_{\text{Fermilab}} \simeq 16.5 \sin^2 2\theta (\text{kton } 10^{19} \text{ pot})^{-1} \quad (18)$$

$$\left(\frac{N_\tau}{N_p}\right)_{\text{CERN}} \simeq 126 \sin^2 2\theta (\text{kton } 10^{19} \text{ pot})^{-1} \quad (19)$$

Using the beam intensity  $N_p/10^{19} = 20$  (3) for Fermilab (CERN) the absolute rates of  $\tau$ -events become:

$$N_\tau(\text{Fermilab}) \simeq 328 \sin^2 2\theta (\text{kton yr})^{-1} \quad (20)$$

$$N_\tau(\text{CERN}) \simeq 383 \sin^2 2\theta (\text{kton yr})^{-1} \quad (21)$$

Note how in this case the lower intensity of the CERN beam is overcompensated by the higher proton energy.

In the low  $|\Delta m^2|$  region the rate of  $\tau$  production for the reference beams for a fixed number of accelerated protons are:

$$\left(\frac{N_\tau}{N_p}\right)_{\text{Fermilab}} \simeq 0.11 \sin^2 2\theta (\Delta m_{-3}^2)^2 (\text{kton } 10^{19} \text{ pot})^{-1} \quad (22)$$

$$\left(\frac{N_\tau}{N_p}\right)_{\text{CERN}} \simeq 0.28 \sin^2 2\theta (\Delta m_{-3}^2)^2 (\text{kton } 10^{19} \text{ pot})^{-1} \quad (23)$$

Using the predicted proton beam intensities the absolute rates of  $\tau$ -events become:

$$N_\tau(\text{Fermilab}) \simeq 2.23 \sin^2 2\theta (\Delta m_{-3}^2)^2 (\text{kton yr})^{-1} \quad (24)$$

$$N_\tau(\text{CERN}) \simeq 0.84 \sin^2 2\theta (\Delta m_{-3}^2)^2 (\text{kton yr})^{-1} \quad (25)$$

For  $|\Delta m^2| \lesssim 10^{-2} \text{ eV}^2$  the oscillation probability  $P \propto E_\nu^{-2}$  depresses the contribution of high energy neutrinos and the softer but more intense Fermilab beam results in a  $\tau$ -rate that is approximately 2.6 times larger than the CERN beam. A realistic comparison between the two projects should take into account the energy spectrum of the produced  $\tau$  leptons, and take into account the detection efficiency and sources of background.

In fig. 4 we show the energy distribution of the interacting  $\nu_\tau$  neutrinos for the Fermilab and CERN LBL projects. We have made two hypothesis for the  $\nu$ -oscillation parameters:

1.  $\Delta m^2 = 3 \times 10^{-3} \text{ eV}^2$  and  $\sin^2 2\theta = 1$ ,
2.  $\Delta m^2 = 10^{-2} \text{ eV}^2$  and  $\sin^2 2\theta = 0.09$ .

The product  $(\Delta m^2)^2 \sin^2 2\theta$  is equal for both choices of parameters. This results in spectra of  $\tau$  leptons that are approximately equal in shape and normalization. For large  $E_\nu$  the spectra are identical, and only approaching the energy threshold the oscillation probabilities for the two cases begin to differ appreciably. The integrated rates for  $\tau$  production rate in units of  $(\text{kton yr})^{-1}$  are 19.6 and 15.8 for the Fermilab beam and 7.5 and 6.9 for the CERN beam. Most of the difference is accumulated at low energies where the efficiency for identification is smaller and it will be very difficult to discriminate between the two sets of parameters discussed in this example. Note that both values of  $|\Delta m^2|$  chosen in our examples are larger than the best fit point of Super-Kamiokande. For lower values of  $|\Delta m^2|$  the *shape* of the energy distribution of the  $\tau$ -events becomes constant. In summary the energy spectrum of the  $\nu_\tau$ 's at the far detector for all values of  $|\Delta m^2| \lesssim 10^{-2} \text{ eV}^2$  (that is in the region indicated by Super-Kamiokande) is well described with the asymptotic form

$$\frac{dN_{\nu_\tau}}{dE_\nu}(E_\nu) = \sin^2 2\theta (\Delta m^2)^2 \frac{L^2}{16} \frac{\phi_{\nu_\mu}^0(E_\nu)}{E_\nu^2} \quad (26)$$

that has a shape independent from the oscillation parameters. The measurement of the absolute value of the rate of  $\tau$  production does measure the product  $(\Delta m^2)^2 \sin^2 2\theta$ . The measurement of the shape of the energy spectrum of the  $\tau$ 's produced in the detector can confirm that indeed the probability of flavor conversion has the energy dependence predicted by the theory, but this prediction is unique. The only information on the parameters is obtained from the absolute normalization.

Is the predicted rate of  $\tau$  events measurable? The strategy for the detection of the signal must find the right balance between mass and resolution. In general the number of detected  $\tau$ 's can be written as:

$$N_\tau^{det} = (\sin^2 2\theta |\Delta m^2|^2) M t N_p \frac{n_\tau^0}{N_p} \langle \epsilon_{det} \rangle \quad (27)$$

Where  $M$  is the detector mass,  $t$  the running time,  $N_p$  the proton beam average intensity,  $n_\tau^0$  (defined in equation (16)) depends on the details of the design of the beam line, and  $\langle \epsilon_{det} \rangle$  is the detection efficiency averaged over the  $\nu_\tau$  energy spectrum.

As concrete example of an experiment the capability to identify  $\nu_\tau$  interactions on an event by event basis we can consider the OPERA [14] and ICARUS [15] detectors<sup>4</sup>. The OPERA detector is based on a sandwich (iron/emulsion/drift/emulsion) of thin ( $\sim 1 \text{ mm}$ ) iron plates alternated with emulsion sheets for high resolution tracking and layers ( $\sim 2.5 \text{ mm}$ ) of 'drift space' filled with a very low density material. Events where a  $\tau$  lepton is produced and decays in the first drift space after the vertex can be identified measuring

---

<sup>4</sup>This is not a comprehensive review of the existing proposals. A more complete discussion should include a discussion of detectors such as NOE and MINOS that have larger mass and coarser resolution.

the direction(s) of the charged decay product(s) in the following layers of emulsions. All  $\tau$  decay modes are observable, and the overall detection efficiency taking (most of the inefficiency is due to  $\tau$ 's that decay inside the iron) is estimated as  $\epsilon_d \simeq 0.35$ . A possible mass is  $M \simeq 0.75$  kton. OPERA running at CERN could detect in 5 years a number of  $\tau$ 's:

$$\begin{aligned} N_{\tau}^{det}(\text{OPERA}) &= (\sin^2 2\theta |\Delta m_{-3}^2|^2) 0.75 \times 5 \times 3 \times 0.28 \times 0.35 \\ &= (\sin^2 2\theta |\Delta m_{-3}^2|^2) 1.1 \end{aligned} \quad (28)$$

with a background smaller than a single event. For the best fit point of Super-Kamiokande the signal predicted by equation (28) corresponds to 4.8 events, for  $|\Delta m^2|/10^{-3} \text{ eV}^2 = 0.5$  (6) (the 90% C.L. interval estimate by SK) to (0.28) (40) events. In the first line of equation (28) we have written explicitly the estimates of the most important quantities that we have used for the prediction. A more intense proton beam, a better optimization of the focusing system, and a higher detection efficiency are all direction of improvement not only possible but actively pursued. Formula (28) can of course be easily rescaled. Qualitatively, we can conclude that a 5-years long dedicated effort based on this emulsion-based vertex detection technique can detect a  $\tau$  signal (if  $\nu_{\mu} \rightarrow \nu_{\tau}$  oscillations are indeed the cause of the Super-Kamiokande data) in most but very likely not all the region of parameter space indicated by the atmospheric neutrino data.

The ICARUS detector is based on a new technology that allows to obtain high resolution ('bubble-chamber quality') images of the 3-D deposition of ionization in a large volume of liquid argon. This detector will not have the spatial resolution to detect the  $\tau$  decay vertex, however the decay mode  $\tau^{-} \rightarrow \nu_{\tau} \bar{\nu}_e e^{-}$  (with a branching ratio of 18%) can be detected with negligible background identifying the electron and the missing transverse momentum due to the two neutrinos in the final state. The overall efficiency can be roughly estimated as  $\langle \epsilon_{det} \rangle \sim 0.18 \times 0.45 \simeq 0.08$ . The lower efficiency with respect to OPERA will be compensated by the larger mass for  $M \gtrsim 3.2$  kton.

Higher mass, lower resolution detectors appear not very likely to have a higher sensitivity than the examples we have discussed.

What is the conclusion of this discussion ? If the strategy to develop a high energy long-baseline neutrino beam and search for the appearance of charged current interactions of  $\nu_{\tau}$ 's sufficiently promising to deserve the very high investment in human and financial resources that are required ? We will leave the reader to make her/his own judgement.

## 4 Disappearance Experiments

The threshold for the charged current interaction of  $\nu_{\tau}$  on free neutrons is  $E_t = 3.47$  GeV (a little higher for bound nucleons). At low energy the cross section is strongly suppressed by kinematical effects and effectively only  $\nu_{\tau}$  with energy  $E_{\nu} \gtrsim 4\text{--}5$  GeV can effectively interact via the charged current interactions. For  $|\Delta m^2|$  in the confidence interval of Super-Kamiokande and the path-length under discussion, the oscillation probability of the neutrinos well above threshold is small and appearance experiments are difficult.

The oscillation probability (for a fixed  $L$ ) reaches a maximum for a discrete set of values of the neutrino energy. For the K2K (Fermilab/CERN) project these values are  $E_\nu = 0.20/n \Delta m_{23}^2$  GeV ( $E_\nu = 0.59/n \Delta m_{23}^2$  GeV) where  $n$  is a positive integer. For maximal mixing the flux of  $\nu_\mu$ 's at these energies will vanish. In the SK 90% confidence interval  $\Delta m_{23}^2 \leq 6$  these energies are always below the threshold and it is natural to explore the possibility to measure the oscillation probability at low energy.

The  $\nu_\tau$  that are below threshold cannot have a charged current interaction, they 'disappear'. This 'disappearance' can be detected observing a deformation of the energy spectrum of the CC interactions, or measuring a ratio  $N(\text{nc})/N(\text{cc})$  of the numbers of neutral and charged current events larger than expectations. This program appears straightforward but it is not easy to put in practice. We can list some of the problems of the experimental strategy.

(1) It is difficult to construct a neutrino flux that is sufficiently intense at low energy. The neutrino flux at the far detector is proportional (see section 2.2) to a factor  $(p_{\perp\nu}/E_\nu)^2$  because the neutrinos are emitted in a cone that shrinks with increasing energy. An appropriate optimization of the focusing system[16, 17] can increase the low energy flux reducing the angular divergence of the charged mesons of low energy<sup>5</sup> however the transverse momentum due to the parent decay cannot be avoided. In a 'standard' design of the beam line the approximation of the 'perfect focusing' (see fig. 5 and the discussions in section 2.2 and in the appendix) is the highest obtainable flux. It is possible that even this maximum flux has an intensity below what is necessary to explore the entire SK confidence interval. Perhaps a very innovative design of the neutrino beam line with a 'thick' target that allows the reinteraction of high energy secondary particles transforming the energy of the primary protons in a large number of low energy pions could result in a much higher flux of low energy neutrinos, but this idea has not yet been explored in any detail.

(2). The method of measuring the ratio NC/CC of neutral current and charged current events becomes increasingly difficult for  $E_\nu \lesssim 1$  GeV where the lowest multiplicity channels (elastic, quasi-elastic, single pion production) are dominant and the theoretical uncertainties large.

(3) The energy spectrum of the interacting neutrinos in the low energy region will be changing rapidly  $\propto E_\nu^2$ , and the deformations of the spectrum not easy to measure.

(4) The systematic uncertainties about the no-oscillation flux, the background sources and the detector response could become a limitation in the sensitivity of the technique. A near detector appears to be essential to reduce these systematic uncertainties to the desired levels. However some systematic effects are likely to remain even in a far/near comparison. The two detectors cannot be identical, and in the near detector only events in a sufficiently small region close to the beam axis should be considered.

The sensitivity of the KEK to Kamioka project [4] is based on the disappearance method, since essentially all the neutrinos produced by the 12 GeV proton beam will be below the threshold for  $\tau$  production. The experiment is expected to start taking data

---

<sup>5</sup>The low energy mesons are 'over-focused' in the reference designs of the Fermilab and CERN designs.

in january 1999, years ahead of the Fermilab and CERN beams. The neutrino mass interval that can be excluded at 90% confidence level after 3 years of running if no signal is observed is  $|\Delta m^2| \lesssim 3 \times 10^{-3} \text{ eV}^2$ .

## 5 Sensitivity of atmospheric neutrino experiments

The ‘atmospheric neutrino anomaly’ has initially appeared as the measurement of a ratio  $R_{\mu/e}$  of  $\mu$ -like and  $e$ -like events lower than the MC expectation. The scientific community remained very skeptical, after all  $R$  is a single number and particle identification a non-trivial task. With the measurement of higher energy events (the multi-GeV sample of Kamiokande)<sup>6</sup> and larger statistical samples (22.5 kton of fiducial mass of Super-Kamiokande) it has been possible to detect *patterns* in the energy and zenith angle distributions of the events that are precisely those expected in the case of neutrino oscillations.

With the detection of these patterns the hypothesis that oscillations are the explanation of the data has become much more convincing. It is in fact difficult to imagine what combination of systematic effects could produce the energy-dependent up-down asymmetry observed by Super-Kamiokande for the  $\mu$ -like events. In fact until now no alternative explanation (besides neutrino oscillations) has been offered for these effects.

The patterns of the distortions of the energy and zenith angle distributions of the detected events have to be estimated comparing the data with a theoretical prediction, and one has to consider carefully the uncertainty in the no-oscillation predictions. However theoretical uncertainties are not expected to be the dominant source of systematic errors. Two very simple and very solid predictions for the neutrino flux in the absence of oscillations: the flavor ratio  $\nu_\mu/\nu_e \simeq 2$ , and the up-down symmetry (equations (1) and (2)) eliminate most of the systematic uncertainty about the prediction.

In the case of  $\nu_\mu \leftrightarrow \nu_\tau$  oscillations the oscillation probability depends only on the ratio  $L/E_\nu$ , and perhaps the most physically intuitive and transparent method to analyse the data is to study the distribution of events as a function of  $L/E_\nu$ . This method has been discussed in the past and recently vigorously advocated by Picchi and Pietropaolo in ref.[18].

In the presence of oscillations the distribution of events as a function of  $L/E_\nu$  is distorted by a factor that is simply the oscillation probability (eq.1). In any experiment the finite resolutions in the measurement of the neutrino energy and path-length smear the measured distribution  $dN/d(L/E_\nu)$  and partially wash-out the sinusoidal pattern of the oscillations.

In the upper panel of fig. 6 we show a montecarlo calculation of the distribution of  $L/E_\nu$  for the charged current interactions of muon neutrinos and antineutrinos (with a cut  $p_\mu \geq 0.5 \text{ GeV}$ ) at the Kamioka mine location. The solid line is the prediction in the absence of oscillations, the dashed line is the expectation in the presence of  $\nu_\mu \leftrightarrow \nu_\tau$

---

<sup>6</sup>The reason why the oscillation patterns are more easily recognizable for higher energy events is mostly due to the fact that the direction of the incident neutrino is better measured because the detected charged lepton is emitted in a cone that shrinks with increasing energy.



oscillations with maximal mixing and  $|\Delta m^2| = 10^{-3} \text{ eV}^2$ . The plot is calculated for a ‘perfect detector’ assuming that the energy and direction of each neutrino is reconstructed with infinite precision. Even in this case however the neutrino path-length  $L$  is not perfectly measured because the neutrino creation point is not known. For each event the oscillation probability is calculated using the neutrino energy and the ‘true’  $L$  generated including fluctuations [20] in the position of the  $\nu$  creation point. To each event is then assigned a ‘reconstructed’ value of the path-length that is the most likely value of  $L$  for a given zenith angle.

In the lower panel of fig. 6 we show the ratio of the oscillated plot to the no-oscillation hypothesis as a function of  $L/E_\nu$  in a restricted interesting range. The features of the oscillation phenomenon are unmistakable and the measurement of its parameters straightforward.

Fig. 6 represents of course an ideal case. In any realistic detector the experimental resolutions will partially wash-out the spectacular pattern. A more realistic example, that is a rough approximation of Super-Kamiokande is shown in fig. 7. We have selected ‘single ring events contained’ events (always with the cut  $p_\mu \geq 2 \text{ GeV}$ ), using the Cherenkov threshold for charged particle detection, and the geometry of the detector and the muon range in water for the containment, and estimated the energy and direction of the neutrino with  $\Omega_\nu = \Omega_\mu$  and  $E_\nu = E_\mu$  (we have neglected the error measurement in  $E_\mu$  and  $\Omega_\mu$ , since the resolutions are smaller than the intrinsic fluctuations due to the production cross section this is a reasonable approximation). One can see that in this case the oscillation patterns are less spectacular than in the ideal case but nonetheless quite clear.

Note that after the inclusion of the detector resolutions the shape of the suppression factor due to oscillations depends on the minimum muon energy considered  $E_\mu^{\min}$ . With increasing  $E_\mu^{\min}$  the pattern of damped oscillations becomes more clear, because the muon direction is more strictly correlated with the neutrino direction and  $L$  is better determined, however the number of detected events decreases because of the steepness of the atmospheric neutrino energy spectrum. In a complete analysis all events should be included, taking into account the energy dependent experimental resolutions.

Fig. 7 has been calculated considering a very large exposure (approximately 20 years of Super-Kamiokande) in order to show clearly the oscillation patterns. For a lower realistic exposure the statistical fluctuations will be larger and the determination of the oscillation parameters less precise. The claim of ‘evidence’ for neutrino oscillations in atmospheric neutrino data by the Super-Kamiokande collaboration is based on 1.5 years. Additional data should allow a more clear detection of the oscillation patterns and a better determination of the parameters.

Looking at fig. 7, one can note immediately see how the oscillation parameters  $\Delta m^2$  and  $\sin^2 2\theta$  are determined. The suppression factor due to oscillation is unity for small  $L/E_\nu$ , decreases with increasing  $L/E_\nu$ , reaching a minimum at  $L/E_\nu \sim 2\pi/|\Delta m^2|$  and then shows some ‘damped oscillations’ around the average value  $\simeq 1 - \frac{1}{2} \sin^2 2\theta = 0.5$ . These features will be true in general. The path-length of atmospheric neutrinos is in the range  $L \simeq 10\text{--}10^4 \text{ km}$ , and assuming an energy interval  $E_\nu \sim 0.1\text{--}10 \text{ GeV}$  the range of  $L/E_\nu$  is  $\sim 1\text{--}10^5 \text{ km/GeV}$ . Given this very large range of  $L/E_\nu$ , it is possible (at least

in the region  $|\Delta m^2| \simeq 10^{-4} - 10^{-1} \text{ eV}^2$ ) to distinguish three regions of  $L/E_\nu$  depending on  $(|\Delta m^2| L/E_\nu)$  being much smaller, larger or comparable with unity.

1. For small  $L/E_\nu$  the oscillation cannot develop.
2. For large  $L/E_\nu$  range the oscillations are rapid and difficult to see for realistic detector resolutions. The average value of the suppression factor is  $1 - \frac{1}{2} \sin^2 2\theta$ .
3. In the intermediate region the oscillating pattern is more evident. This region is the crucial one for the determination of  $\Delta m^2$ . Of particular importance is the shape of the distribution around the value  $L/E_\nu \sim 2\pi/\Delta m^2$  (corresponding to the point where the oscillation probability has the first maximum). The identification of a maximum in the suppression factor would be at the same time a clear proof of the existence of oscillations and a determination of the  $|\Delta m^2|$  value.

## 5.1 A new detector for atmospheric neutrinos ?

Most of the data on atmospheric neutrinos has been obtained with water Čerenkov detectors. Recently an iron calorimeter, the Soudan-II detector has obtained a result that supports the SK result. However this detector has a fiducial mass of only 0.5 kton and will not be able to collect a very large statistics. The clear confirmation of the atmospheric neutrino anomaly using a different experimental technique is clearly very desirable.

Is it possible to develop a detector for atmospheric neutrinos with the capability not only to confirm the Super-Kamiokande result but to provide a measurement that is at least in some respects of superior quality ? This task is not easy, because of the remarkable qualities of the Super-Kamiokande experiment: very large mass, very good spatial and energy resolutions, isotropic efficiency.

A possible direction is the development of a moderate mass but higher resolution detectors capable for example to measure also the nuclear recoil in quasi-elastic neutrino scattering. The ICARUS [15] detector could have the potential to perform this measurement, however reinteractions in the target nucleus could become the most important source of error in the determination of the energy and direction of the incident neutrino [21].

Recently [18, 19, 16] the potential of a large mass tracking calorimeter for the measurement of atmospheric neutrinos has also been discussed as an attractive possibility. A possible advantage of a calorimeter compared to a water Čerenkov detector is the potential to perform a better measurement of the events with several particles in the final state because of superior pattern recognition capabilities. The possibility to include a magnetic spectrometer [16] for the measurement of the momentum of the muons that exit the detector in the 'semi-contained' events has also been investigated. The optimum design for such a calorimeter (with the right balance between mass and granularity) is still under discussion.

A natural idea is of course to try to do two things at the same time and develop a detector that can at the same time perform a high quality measurement of atmospheric

neutrinos and of the neutrinos of a LBL beam. The idea is attractive, but the design of such a detector is not easy, because the optimization of the detector performance for the two type of measurements can push toward different non-compatible solutions. As an obvious example, the neutrinos from the beam come from a single (horizontal) direction while atmospheric neutrinos are quasi-isotropic, with the vertical axis as the most important direction. The orientation of the elements of the detector is therefore problematic.

## 6 Discussion and conclusions

The discovery of neutrino oscillations could open a precious new window on the physics beyond the standard model. It is therefore necessary to have an independent and unambiguous confirmation of the evidence collected by Super-Kamiokande and supported by other experimental results. The next step is to measure with precision the oscillation parameters.

What is the best strategy to achieve these goals ? Long-baseline neutrino beams have been proposed since several years as a sensitive instrument to perform detailed studies on neutrino oscillations. However the 90% confidence interval obtained by Super-Kamiokande ( $5 \times 10^{-4} < |\Delta m^2| < 6 \times 10^{-3} \text{ eV}^2$ ) is lower than earlier estimates and as a consequence the long baseline experimental programs have become much more difficult and less attractive. Do they remain the wisest experimental strategy for a confirmation and for detailed studies of the phenomena indicated by SK ? The answer is not easy, but this question should be studied in depth because of the intrinsic scientific interest of the problem, and because in any case the new experimental studies will require a very large investment of scarce human and financial resources.

In this work we have briefly discussed three different experimental approaches to the problem:

1. a LBL ‘appearance’ experiment,
2. a LBL ‘disappearance’ experiment,
3. a new atmospheric neutrino experiment.

In a  $\tau$ -appearance experiment the signal is produced by neutrinos above the threshold for  $\tau$  production, that is with  $E_\nu \gtrsim 4\text{--}5 \text{ GeV}$ . For  $|\Delta m^2|$  in the SK confidence interval the probability of oscillations of these neutrinos is always small and the detectable signal difficult to observe. For the ‘reference’ design of the Fermilab (CERN) beam, assuming maximal mixing and  $|\Delta m^2| = 10^{-3} \text{ eV}^2$ , the inclusive rate of  $\tau$  production (assuming  $\epsilon_{det} = 1$ ) is 2.2 (0.84) events/(kton yr). To a very good approximation the signal is proportional to  $\sin^2 2\theta (\Delta m^2)^2$ . Considering the predicted event rate, and realistic estimates of detector mass and efficiency one can conclude that a positive signal can be detected by very sensitive detectors but only in part of the SK confidence interval. Improvements in beam intensity and design, a larger detector mass, higher efficiency and of course more patience in collecting data can push the sensitivity down to lower values of  $|\Delta m^2|$ . However even in the presence of a negligible background, since the signal is  $\propto (\Delta m^2)^2$  the increase in

sensitivity can only come at a high cost.

The feasibility of a disappearance experiment capable of covering the entire Super-Kamiokande confidence interval has not yet been demonstrated and requires additional studies. The main problems are: (i) the design of a neutrino beam with the required intensity in the low energy region; (ii) the demonstration that the systematic uncertainties in the knowledge of the no-oscillation beam and in the detector response can be kept below the required level. The KEK to Kamioka (K2K) project is expected to start taking data in January 1999. In the absence of a positive signal, after 3 years of running, it would exclude at the 90% confidence level the neutrino mass region  $|\Delta m^2| \lesssim 3 \times 10^{-3} \text{ eV}^2$ . The results from K2K can be a very important guide for the other experiments.

If the effects observed in the measurements of atmospheric neutrinos are indeed due to neutrino oscillations, Super-Kamiokande, after the analysis of a larger sample of data, should be able to see more clearly the oscillation patterns, narrowing the confidence interval for the oscillation parameters. The confirmation of these results by an independent experiment of comparable sensitivity and using a different technique is very desirable. The design and construction of a neutrino detector with the capability of performing measurements of atmospheric neutrinos of comparable or superior quality with respect to Super-Kamiokande is not an easy task. The concept of a large mass, high resolution tracking calorimeter is under investigation.

## Acknowledgements

Part of this work was presented by one of us (P.L.) during the Workshop on “Frontier objects in Astrophysics and Particle Physics” held in Vulcano (Italy) in May 1998. This expanded written version was conceived during after session discussions. We wish to thank the organizers of the conference for having provided the stimulating atmosphere. We acknowledge many illuminating discussions with colleagues, that occurred also before and after the conference. In particular we would like to thank U.Dore, A.Ereditato, A.Ferrari, G.Giannini, S.Mikheyev, G.Mannocchi, P.Picchi, F.Pietropaolo, S.Ragazzi, A.Rubbia, R.Santacesaria, E.Scapparone, T.Stanev, M.Spinetti, T.Tabarelli.

## Appendix:

### Analytic calculation of a LBL $\nu$ beam

The detailed calculation of a LBL neutrino beam is a task that can only be performed with detailed montecarlo codes, however to obtain *understanding* about the possible characteristics of a long baseline neutrino beam, it is simple and useful to compute its spectrum analytically. We can start observing that at the detector site the neutrino creations region is well approximated as a point, and the solid angle subtended by the detector  $\Delta\Omega_{det} = A_{det}/L^2 \simeq 10^{-10}$  radians ( $L$  is the neutrino path-length) is small and therefore the neutrinos to a good approximation can be considered as collinear, and we can define a neutrino flux at the detector

$$\phi_\nu(E_\nu) \simeq \frac{\Delta\Omega_{det}}{A_{det}} \left[ \frac{dN_\nu}{dE_\nu d\Omega_\nu}(E_\nu, \Omega_\nu) \right]_{\Omega_\nu=\Omega_{det}} \quad (29)$$

where  $\Omega_\nu$  is the neutrino direction and  $\Omega_{det}$  is the direction of the line of sight from the accelerator to the detector. For a perfect beam design  $\Omega_{det} = \Omega_p \equiv 0$  ( $\Omega_p$  is the proton beam direction).

The dominant source if  $\nu_\mu$  (or  $\bar{\nu}_\mu$  neutrinos is the decay of charged pions and kaons. In general we can write :

$$\begin{aligned} \frac{dN_\nu}{dE_\nu d\Omega_\nu}(E_\nu, \Omega_\nu) &= \sum_{a=\pi, K} B_{a \rightarrow \mu\nu} \int dE_a \int d\Omega_a \frac{dn_a}{dE_a d\Omega_a}(E_a, \Omega_a, E_0) P_{dec}(E_a) \\ &\quad \int d\Omega_{a\nu} \frac{dn_{a \rightarrow \nu}}{dE_\nu d\Omega_{a\nu}}(E_\nu, \Omega_{a\nu}, E_a) \delta[\Omega_\nu - (\Omega_a \oplus \Omega_{a\nu})] \end{aligned} \quad (30)$$

where  $dn_a/(dE_a d\Omega_a)$  is the differential distribution in energy and direction of the parent mesons,  $P_{dec}(E_a)$  is the decay probability,  $dn_{a \rightarrow \nu}/(dE_\nu d\Omega_{a\nu})$  is the distribution in energy and angle (with respect to the parent direction) of the neutrino produced by a primary meson of energy  $E_a$ , and the delta function imposes that the produced neutrino has the desired direction. The neutrino distributions with respect to a parent of given energy and direction are easily obtained, knowing that the  $a \rightarrow \mu\nu$  decay is isotropic in the parent meson rest frame. Using the conservation of 4-momentum:

$$\frac{dn_{a \rightarrow \nu}}{dE_\nu d\Omega_{a\nu}}(E_\nu, \Omega_{a\nu}, E_a) = \frac{1}{4\pi} \int_{-1}^{+1} dz \delta[E_\nu - \gamma p_a^*(1 + \beta z)] \delta \left[ \cos \theta_{a\nu} - \frac{z + \beta}{1 + \beta z} \right] \quad (31)$$

where  $z = \cos \theta^*$  is the cosine of the c.m. decay angle.  $p_a^*$  is the 3-momentum of the decay products in the parent rest frame and  $\gamma$  and  $\beta$  are the Lorentz factor and velocity of the parent meson.

The simplest case is the so called ‘perfect focus’ approximation, that is the assumption that all particles with charge of the correct sign after the focusing system are collinear with the beam. In this case all integrations in equation (30) can be solved using the Dirac

deltas: The solution for the most interesting case of a detector aligned with the proton beam (using for simplicity the expression valid for ultrarelativistic mesons) is :

$$\phi_\nu(E_\nu; E_0, L) = \frac{1}{4\pi L^2} \sum_{a=\pi, K} \frac{B_{a \rightarrow \mu\nu}}{1 - r_a} \left[ \frac{dn_a}{dE_a}(E_a, E_0) \exp\left(-\frac{T m_a}{\tau_a E_a}\right) \right]_{E_a=E_\nu/(1-r_a)} \left(\frac{E_\nu}{p_a^*}\right)^2 \quad (32)$$

where  $r_a = 1 - (m_\mu/m_a)^2$  ( $r_\pi = 0.5731$ , and  $r_K = 0.0458$ ), and  $T$  is the length of the tunnel. Equation (32) has a transparent meaning. A neutrino of energy  $E_\nu$  along the beam direction can be produced only by a parent pion (kaon) of energy  $E_\nu = E_\pi/(1 - r_\pi)$  that decays emitting the neutrino in the forward direction. The flux of neutrinos of energy  $E_\nu$  is therefore given by the number of parent mesons of appropriate energy produced in an interaction, multiplied by the decay probability, and by a Jacobian factor  $(1 - r_a)^{-1} (E_\nu/p_a^*)^2$ , where  $p_a^*$  is the momentum of the neutrino in the rest frame of the parent particle ( $p_\pi^* = 29.8$  MeV,  $p_K^* = 236$  MeV). The Jacobian factor takes into account the facts that the range of neutrino energy is compressed by a factor  $1 - r_a$  with respect to the range of parent mesons, and that the neutrinos are produced in a solid angle that shrinks with increasing energy as  $E_\nu^{-2}$ , correspondingly the neutrino flux at the detector is enhanced by the inverse factor. Comparing the contribution of pions and kaons to the neutrino flux we can notice that the kaon contribution is enhanced because of the shorter lifetime, but depressed because of the larger  $p^*$ . In the decays of pions (kaons) the neutrino can take at most a fraction  $1 - r_\pi = 0.427$  ( $1 - r_K = 0.954$ ) of the parent energy, therefore all neutrinos above the energy  $0.427 E_0$  are produced by kaon decay.

For a detector aligned with the proton beam but for an arbitrary angular distribution of the final state particles the neutrino flux can be obtained with a single integration, for example as:

$$\begin{aligned} \phi_\nu(E_\nu; E_0, L) = & \frac{1}{4\pi L^2} \sum_{a=\pi, K} \frac{B_{a \rightarrow \mu\nu}}{1 - r_a} \int d\cos\theta_a \left[ \frac{d^2 n_a}{d\cos\theta_a dE_a}(E_a, \cos\theta_a; E_0) \right. \\ & \left. P_{dec}(E_a) \left(\frac{2E_a}{p_a^*}\right)^2 \left(\frac{E_\nu}{E_a(1 - r_a)}\right) \right]_{E_a=E_a(E_\nu, \theta_a)} \end{aligned} \quad (33)$$

where

$$E_a(E_\nu, \theta) = \frac{E_\nu}{1 - r_a} \left( \frac{2}{1 + \sqrt{1 - (\theta E_\nu/p_a^*)^2}} \right) \quad (34)$$

is the parent meson energy that can produce a final state neutrino of energy  $E_\nu$  at an angle  $\theta$  with respect to the parent direction.

As far as the calculation of the number of pions and kaons of energy  $E_\pi$  ( $E_K$ ) produced in an interaction by a primary proton of energy  $E_0$  is concerned (see eq. 10), in our analytic calculation, we have used the form  $F(x) = C e^{-ax} (1 - x)^b$  to fit montecarlo generated data.

## References

- [1] Y. Fukuda *et al.* (SuperKamiokande collaboration) preprint hep-ex/9803006 and hep-ex/9805006.
- [2] See for example T. K. Gaisser, in *Neutrino '96*, Proceedings of the 17th Conference on Neutrino Physics and Astrophysics, Helsinki, 1996.
- [3] CHOOZ collaboration: M. Apollonio *et al.*, hep-ex/971102.
- [4] Yuichi Oyama, “K2K (KEK to Kamioka) neutrino-oscillation experiment at KEK-PS” preprint hep-ex/9803014, and <http://ale.physics.sunysb.edu/lbl/lbl.html>.
- [5] NUMI beam <http://www-numi.fnal.gov:8875/numi/beam/spectrum.html>
- [6] C. Acquistapace *et al.*, “The CERN Neutrino beam to Gran Sasso (NGS)” preprint INFN/AE-98/05 (1998).
- [7] P. Lipari, M. Lusignoli, and F. Sartogo, Phys.Rev.Lett. 74, 4384 (1995).
- [8] G. Barr *et al.*, Phys. Rev. D 39, 3532 (1989); V. Agrawal, *et al.*, Phys. Rev. D 53, 1313 (1996); V. Agrawal, T. K. Gaisser, P. Lipari, and T. Stanev, Phys. Rev. D 53 1314, (1996).
- [9] M. Honda, T. Kajita, K. Kasahara, and S. Midorikawa, Phys. Rev. D 52, 4985 (1995);
- [10] Kamiokande collaboration: K.S. Hirata *et al.* Phys. Lett. B 205, 416 (1988), *ibid.* 280, 146 (1992); Y. Fukuda *et al.* Phys. Lett. B 335, 237 (1994).
- [11] G. Battistoni *et al.*, to appear in the Proceedings of TAUP 97, LNGS, and private communication.
- [12] Paolo Lipari, T. K. Gaisser and Todor Stanev preprint astro-ph/9803093.
- [13] T. K. Gaisser, M. Honda, K. Kasahara, H. Lee, S. Midorikawa, V. Naumova and Todor Stanev Phys.Rev. D 54, 5578 (1996) (hep-ph/9608253)
- [14] H.Shibuya *et al.* “The OPERA emulsion detector for a long-baseline neutrino-oscillation experiment.” Letter of intent LNGS-LOI 8/97.
- [15] P.Cennini “ICARUS II. A second generation Proton Decay Experiment and Neutrino Observatory at the Gran Sasso Laboratory”. Experiment Proposal LNGS-94/99-I and 99-II (1994). J.P. Revol *et al.* “A Search Programme for Explicit Neutrino Oscillations at Long and Medium Baselines with ICARUS detector”. ICARUS-TM-97/01 (1997).
- [16] M. Apollonio *et al.*, “Expression of Interest for a long baseline accelerator and atmospheric neutrino oscillation experiment at Gran Sasso”, presented to the International Scientific Committee of the Gran Sasso Laboratory, unpublished.

- [17] M. Apollonio et al., “Studies for a long baseline accelerator and atmospheric neutrino oscillation experiment at Gran Sasso”, presented to the International Scientific Committee of the Gran Sasso Laboratory, unpublished.
- [18] P. Picchi and F. Pietropaolo ICGF Rapp.Int. 344/1977; G. Mannocchi et al., preprint hep-ph/9801339 (1998).
- [19] A. Curioni et al., preprint hep-ph/9805249 (1998)
- [20] T. K. Gaisser and Todor Stanev, preprint astro-ph/9708146.
- [21] G. Battistoni, P. Lipari, J. Ranft and E. Scapparone, preprint hep-ph/9801426 and LNGS preprint INFN/AE-98/03



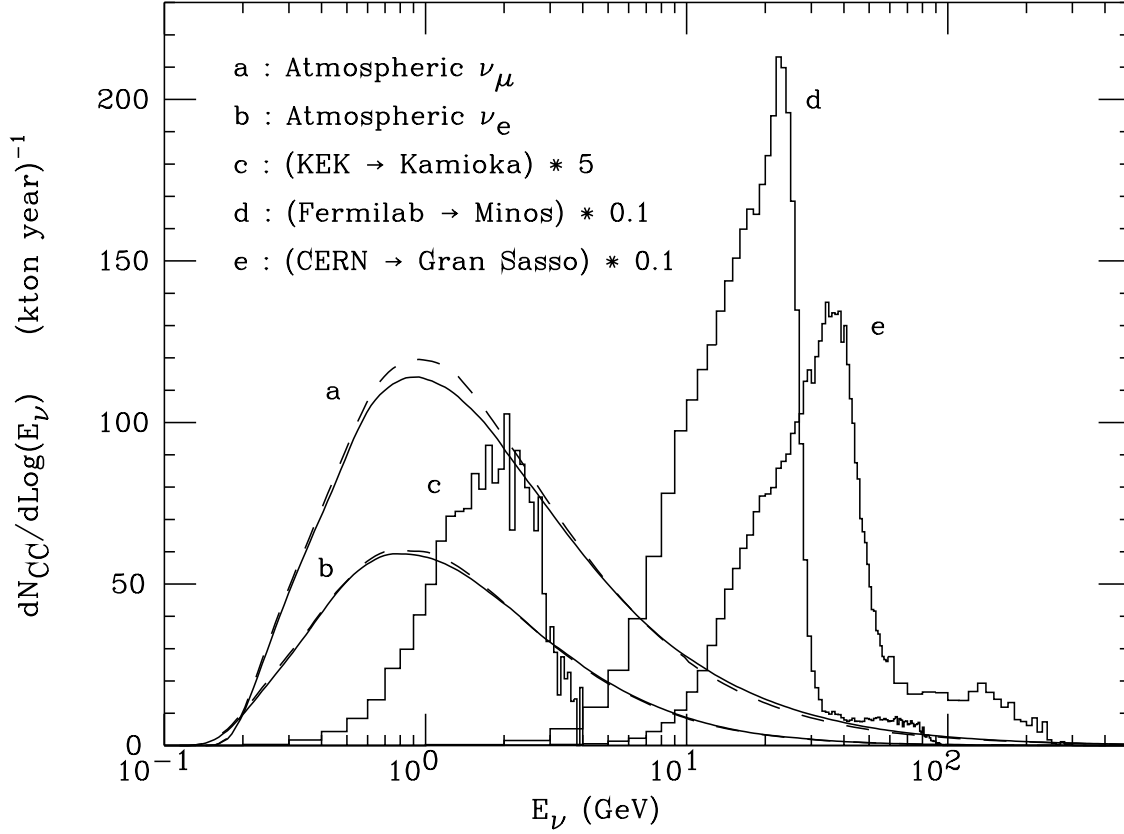


Figure 1: Energy distribution of interacting (with charged current) atmospheric neutrinos and antineutrinos, and of the  $\nu_\mu$  in three LBL experiments. All calculations assume the absence of neutrino oscillations. For atmospheric neutrinos the solid (dashed) lines are calculated with the the Bartol [8] (Honda et al. [9]) The scale of the vertical axis is absolute, note however that the LBL fluxes are multiplied by constant factors.

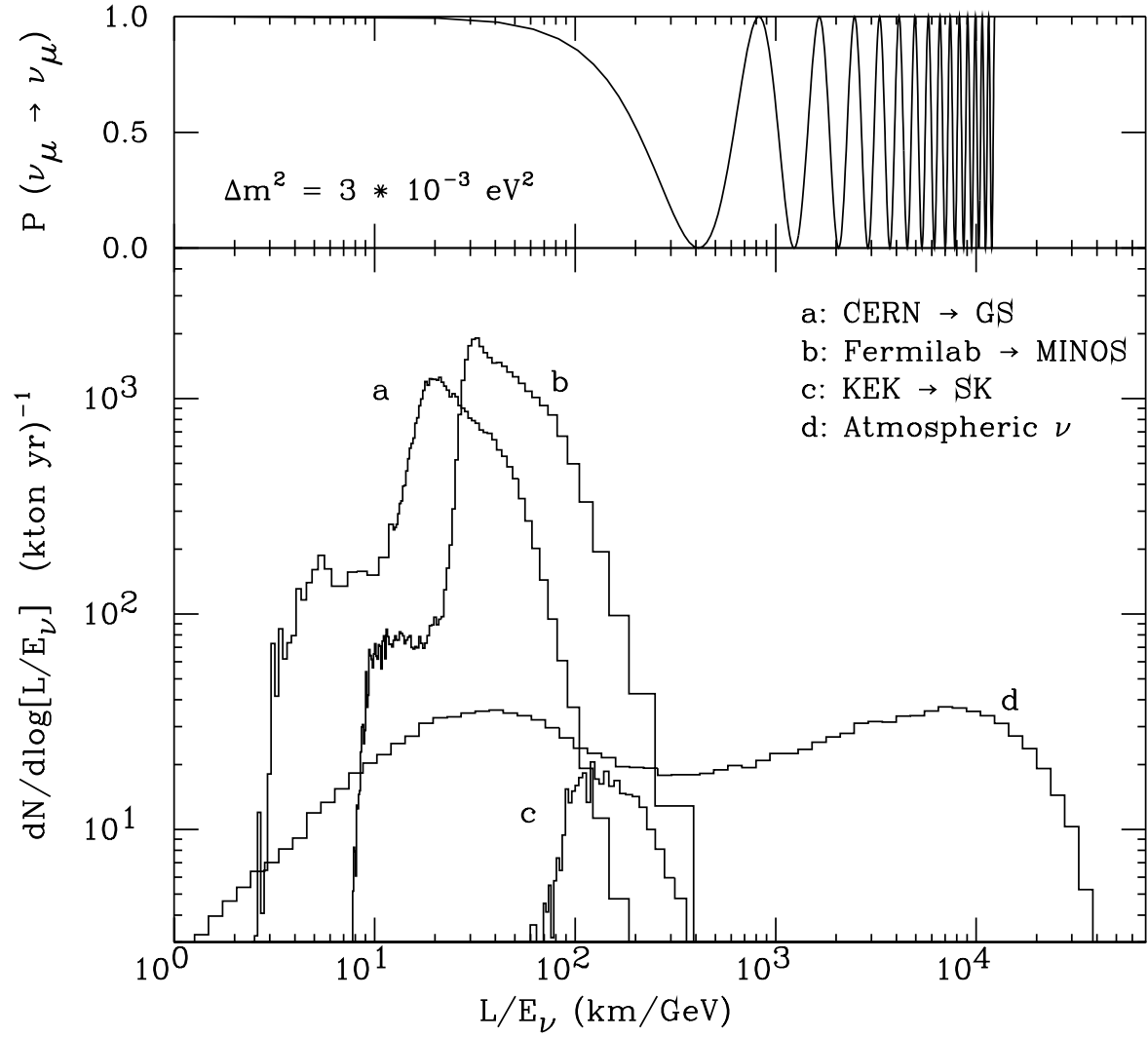


Figure 2: Distribution in  $L/E_\nu$  of the charged current events expected (in the absence of oscillations) in three LBL experiments, and for atmospheric neutrinos with a cut  $p_\mu \geq 0.2$  GeV. In the upper panel we show the oscillation probability for maximal mixing and  $\Delta m^2 = 3 \times 10^{-3} \text{ eV}^2$ .

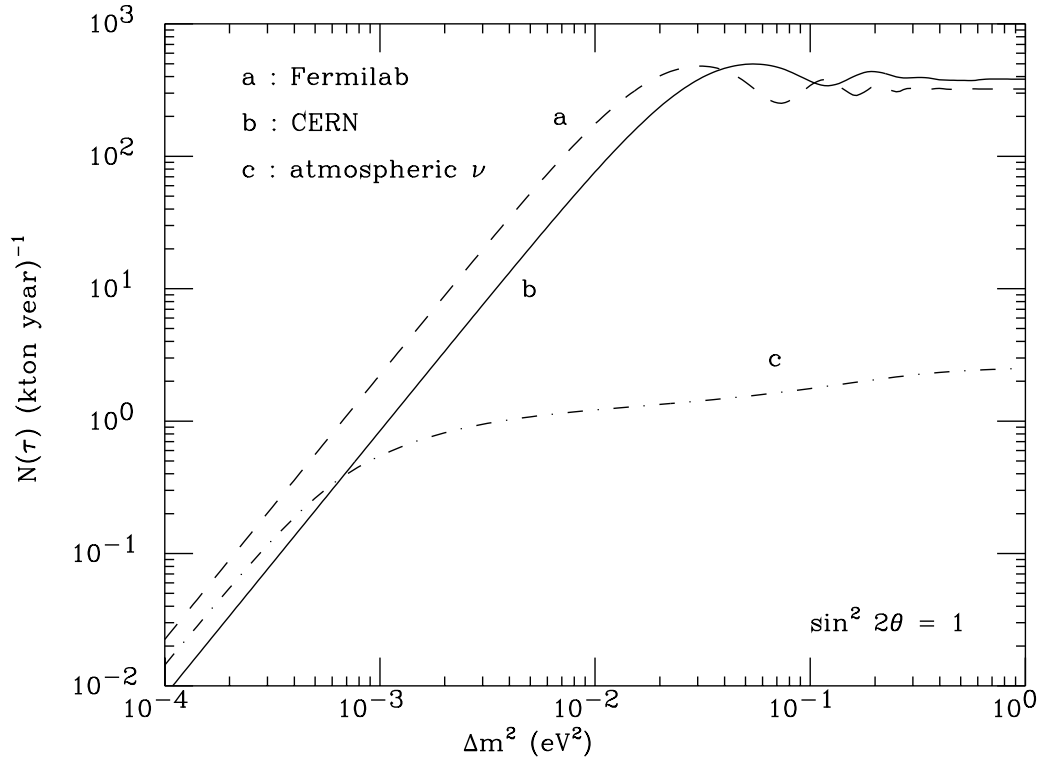


Figure 3: Rate of  $\tau$  lepton production as a function of  $\Delta m^2$  assuming maximal mixing  $\nu_\mu \leftrightarrow \nu_\tau$  oscillations.

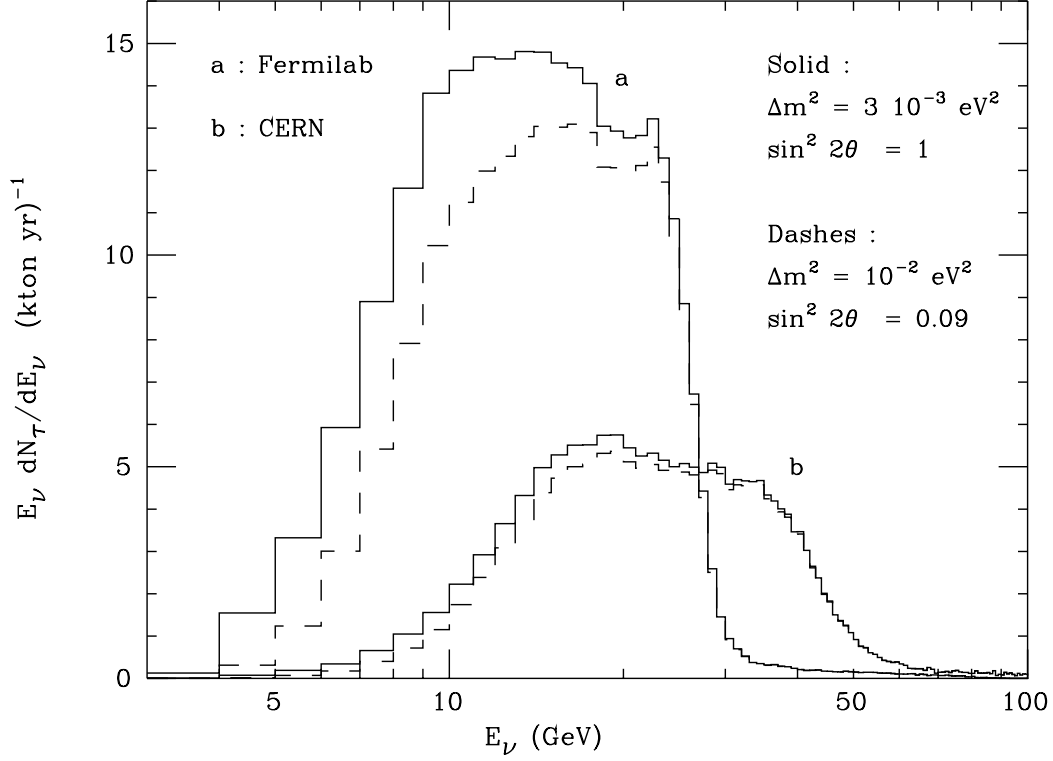


Figure 4:  $dN/d\text{Log}E_\tau$  distribution of the  $\nu_\tau$ 's interacting via charged current for the Fermilab to Minos and the CERN to Gran Sasso LBL neutrino beams. The distributions are calculated assuming the existence of  $\nu_\mu \leftrightarrow \nu_\tau$  oscillations with  $\Delta m^2 = 3 \times 10^{-3} \text{ eV}^2$  and  $\sin^2 2\theta = 1$  (solid histograms) and  $\Delta m^2 = 10^{-2} \text{ eV}^2$  and  $\sin^2 2\theta = 0.09$ . The absolute scale is in  $(\text{kton yr})^{-1}$ , assuming a number of protons of target of  $2 \times 10^{20}$  and  $3 \times 10^{19}$  for the two LBL beams.

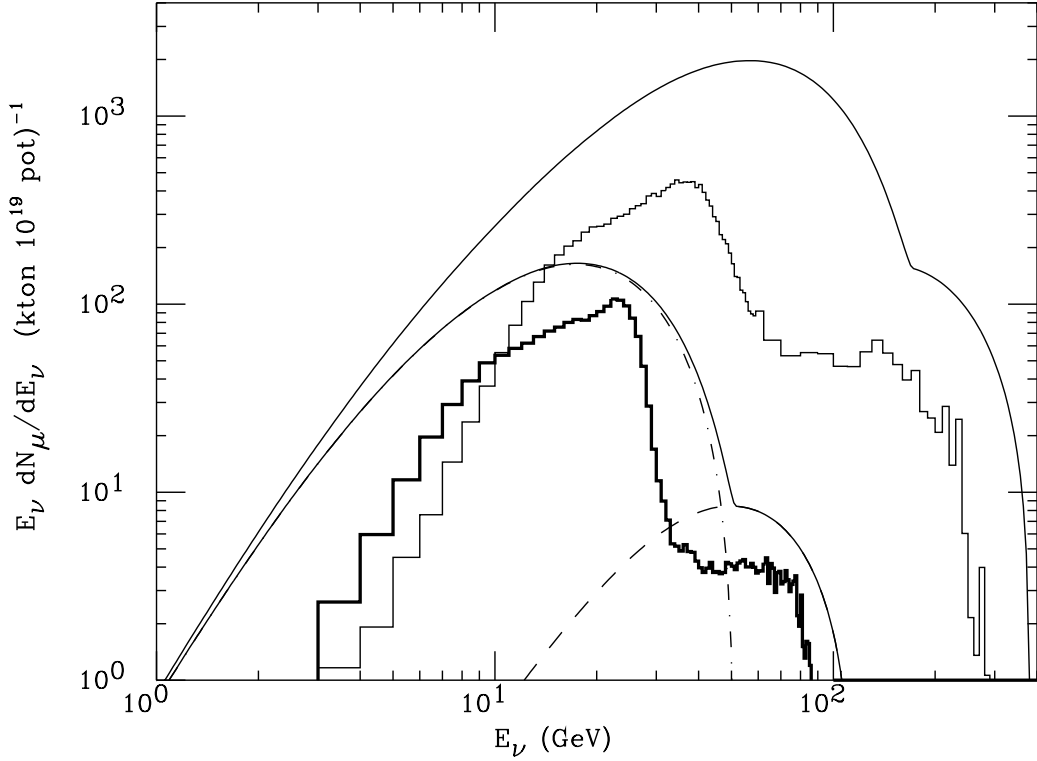


Figure 5: Energy distribution of the interacting neutrinos (charged current interactions) for the Fermilab to Minos (thick histogram) and CERN to Gran Sasso (thin histogram) LBL beams, compared with an analytic approximation under the assumption of perfect focusing. The energy of the proton beam is 120 and 400 GeV for the two cases. The absolute scale of the rate is per kiloton and for a fixed number ( $10^{19}$ ) accelerated protons on target.

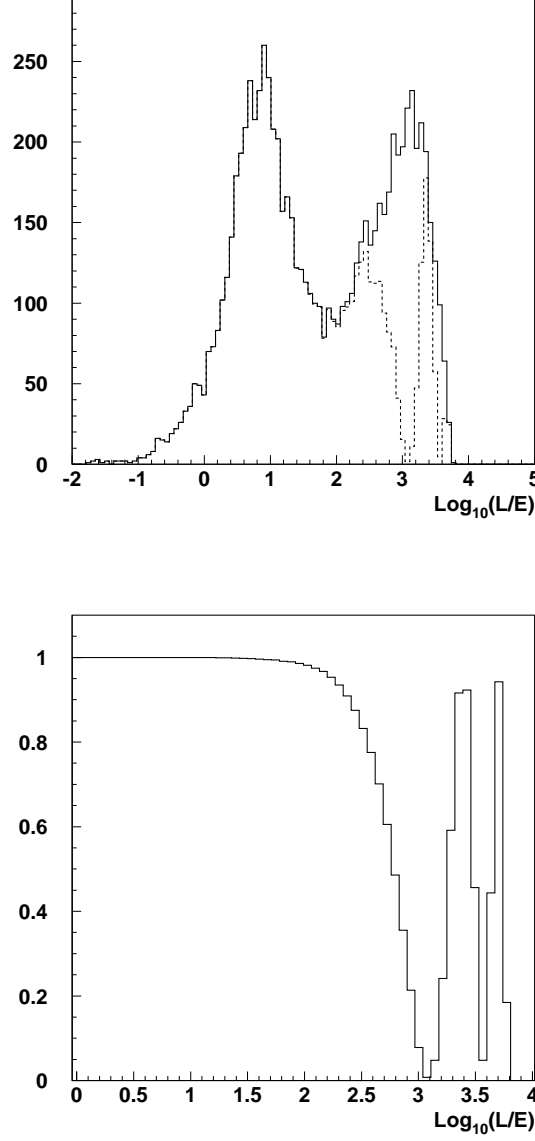


Figure 6: Upper panel: distribution in  $L/E_\nu$ , in units of km/GeV, of the charged current  $\nu_\mu$  and  $\bar{\nu}_\mu$  events expected for atmospheric neutrinos with a cut  $p_\mu \geq 2.0$  GeV at the Kamioka site. The solid line corresponds to no oscillation hypothesis, the dotted line is the expectation for maximal mixing and  $\Delta m^2 = 10^{-3}$ . We are assuming exact knowledge of the direction and energy of the neutrinos; only fluctuations in the position of the neutrino creation point are contributing to the resolution in  $L/E_\nu$ . Lower panel: ratio of the oscillation case to the no-oscillation hypothesis as a function of  $L/E_\nu$ .

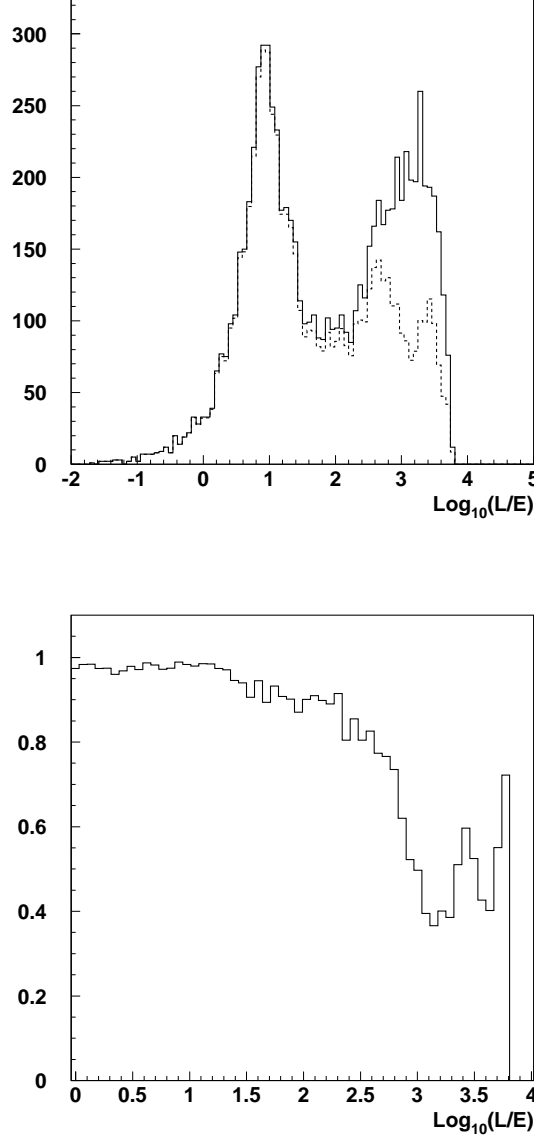


Figure 7: Upper panel: distribution in  $L/E_\nu$ , in units of km/GeV, of the charged current  $\nu_\mu$  and  $\bar{\nu}_\mu$  events expected for atmospheric neutrinos with a cut  $p_\mu \geq 2.0$  GeV at the Kamioka site. The solid line corresponds to no oscillation hypothesis, the dotted line is the expectation for maximal mixing and  $\Delta m^2 = 10^{-3}$ . The direction and energy of the neutrino are estimated as  $E_\nu \simeq E_\mu$  and  $\Omega_\nu = \Omega_\mu$ . The statistics of the montecarlo calculation corresponds to the large exposure of 500 (kton yr). Lower panel: ratio of the oscillation case to the no-oscillation hypothesis as a function of  $L/E_\nu$ .